Least squares realization of complex-valued multiple-output autonomous LTI systems via the Riemannian singular value decomposition

Sem Viroux, Sibren Lagauw, Bart De Moor *Fellow, IEEE & IFAC & SIAM*

***Abstract*— This paper presents a generalization of least squares realization of multiple-output linear time-invariant (LTI) models to the complex field, thereby enabling broader applicability in areas such as signal processing and control theory. We discuss the challenges inherent to optimization over complex variables and formulate the realization problem as a structured total least squares (STLS) problem. A key contribution is the derivation of a nonlinear generalized singular value decomposition (SVD) over the complex domain. We adapt an existing heuristic algorithm that works over the real domain to solve the complex nonlinear generalized SVD. We validate our framework through illustrative examples and demonstrate its use in a nuclear magnetic resonance (NMR) modeling problem and a direction of arrival (DOA) estimation problem.**

I. Introduction

We consider *complex-valued multiple-output autonomous linear time-invariant (LTI) causal lumped parameter dynamical models in discrete-time, with a pre-specified model order* n. The output data $\widehat{\boldsymbol{y}}_i = [\widehat{y}_{i,0} \ \cdots \ \widehat{y}_{i,N-1}]^{\mathsf{T}} \in \mathbb{C}^N$ (with $N > n$) satisfy a difference equation of the form:

$$\widehat{y}_{i,k+n} + a_1\widehat{y}_{i,k+n-1} + \cdots + a_n\widehat{y}_{i,k} = \boldsymbol{a}(z)\widehat{y}_{i,k} = 0, \quad (1)$$

where $\widehat{\boldsymbol{y}}_i$ is the ith output signals and $\boldsymbol{a}(z) = z^n + a_1 z^{n-1} + \cdots + a_n$ is a degree n polynomial in the forward-shift operator z (i.e., $zy_{i,k} = y_{i,k+1}$), the coefficients of which correspond to the parameters $\boldsymbol{a}_{\mathrm{tr}} = [a_n \ a_{n-1} \ \cdots \ a_1]^{\mathsf{T}} \in \mathbb{C}^n$ of the (complex-valued) multiple-output LTI model. The data $\widehat{\boldsymbol{y}}_i$ are said to be *model-compliant* since they satisfy difference equation (1) for all $k = 0, \ldots, N-n-1$.

Suppose we are given p sequences of data $\boldsymbol{y}_i \in \mathbb{C}^N$ that do not comply with (1). We want to find the model-compliant output sequences $\widehat{\boldsymbol{y}}_i$ that (in a least squares (LS) sense) best approximate the *given data* $\boldsymbol{y}_i$, by minimizing the *misfits* $\widetilde{\boldsymbol{y}}_i = \boldsymbol{y}_i - \widehat{\boldsymbol{y}}_i$. This modeling setup is depicted in Fig. 1.

$$\underset{\substack{\widehat{\boldsymbol{y}}_1,\ldots,\widehat{\boldsymbol{y}}_p \in \mathbb{C}^N \\ \boldsymbol{a}_{\mathrm{tr}} \in \mathbb{C}^n}}{\text{minimize}} \quad \frac{1}{2}\sum_{i=1}^{p} \|\widetilde{\boldsymbol{y}}_i\|_2^2 = \frac{1}{2}\sum_{i=1}^{p} \|\boldsymbol{y}_i - \widehat{\boldsymbol{y}}_i\|_2^2, \quad (2a)$$

$$\text{subject to} \quad \boldsymbol{a}(z)\widehat{y}_{i,k} = 0, \ k = 0, \ldots, N-n-1. \quad (2b)$$

Sem Viroux (corresponding author), Sibren Lagauw and Bart De Moor are with the Center for Dynamical Systems, Signal Processing, and Data Analytics (STADIUS), Dept. of Electrical Engineering (ESAT), KU Leuven. Kasteelpark Arenberg 10, B-3001 Leuven, Belgium. E-mail addresses: {sem.viroux, sibren.lagauw, bart.demoor}@kuleuven.be

This work was supported in part by the KU Leuven: Research Fund (project iBOF/23/064), and several LRD bilateral industrial projects; in part by Flemish Government agencies: EWI (Flanders AI Research Program), FWO (the work of S. Lagauw was supported by the FWO Fundamental Research PhD Fellowship under grant 11K5625N), and in part by the European Research Council (ERC) under the European Union's Horizon 2020 research and innovation programme (ERC Adv. Grant No 885682).

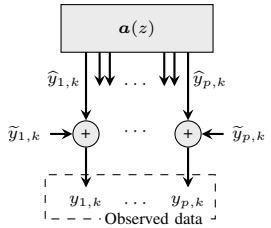

Fig. 1. Schematic overview of the autonomous LTI multiple-output model. The given output data $\boldsymbol{y}_i \in \mathbb{C}^N$ are modified using the so-called misfits $\widetilde{\boldsymbol{y}}_i \in \mathbb{C}^N$, so that the modified data $\widehat{\boldsymbol{y}}_i \in \mathbb{C}^N$ are model-compliant. The coefficients $\boldsymbol{a}_{\mathrm{tr}} \in \mathbb{C}^n$ of the nth degree polynomial $\boldsymbol{a}(z)$ in the forward-shift operator z, are the unknown model parameters.

This type of realization problem is well-known in the literature, and has been studied extensively for real-valued data and model parameters [1]–[3]. However, systems theory is not inherently limited to real-valued signals and/or models, see e.g., the framework presented in [4]; digital communication applications [5]; nuclear magnetic resonance (NMR) modeling [6]; or rotor bearing systems identification [7]. More recently, the use of complex-valued signals has also gained prominence in the neural network community [8], making the topic increasingly relevant.

In addition to its application in system identification [9], this problem framework also appears in contexts such as *direction of arrival (DOA)* estimation in array processing; see e.g., [10] and the references therein. Furthermore, the body of related literature is large since this system identification problem corresponds to a particular instance of a structured low rank approximation problem: *structured total least squares (STLS)*, see e.g., [11]–[13].

Our contributions are twofold. First, while the presented methodology shares similarities with the existing literature [11]–[13], it differs fundamentally in the following way: unlike previous work, we consider complex-valued signals, and consequently allow our model to be described by a linear homogeneous difference equation with constant *complex-valued* coefficients. This allows for a broader class of applications, including frequency estimation, in which complex signals occur naturally [5]. Second, the proposed framework provides a systematic approach for generalizing other types of STLS problems to a complex-valued setting.

Outline: We address the key intricacies associated with optimization over complex decision variables in Section II. We characterize first-order optimality and derive a nonlinear generalized singular value decomposition (coined Rieman-

nian SVD) in the complex field (Section III), followed by an extension of the variable metric inverse iteration algorithm to the complex domain (Section IV). We work out several numerical examples in Section V to validate the proposed methodology, demonstrating its use in a NMR modeling and a DOA estimation problem.

Notation: We denote scalars by lowercase letters, e.g., a, and tuples/vectors by boldface lowercase letters, e.g., $\boldsymbol{a}$. Matrices are characterized by boldface uppercase letters, e.g., $\boldsymbol{A}$. We use j to denote the imaginary unit $\sqrt{-1}$. The complex conjugate, transpose, and Hermitian transpose of $\boldsymbol{x} \in \mathbb{C}^d$ are indicated by $\overline{\boldsymbol{x}}$, $\boldsymbol{x}^{\mathsf{T}}$, and $\boldsymbol{x}^{\mathsf{H}}$, respectively. The real and imaginary parts are denoted by $\boldsymbol{x}^{\mathrm{Re}}, \boldsymbol{x}^{\mathrm{Im}} \in \mathbb{R}^d$, respectively, such that $\boldsymbol{x} = \boldsymbol{x}^{\mathrm{Re}} + \mathrm{j}\boldsymbol{x}^{\mathrm{Im}}$. Subscript i and k of the given data, model-compiant data, and misfit respectively denote the output and time indices, e.g., $y_{i,k}$, $\widehat{y}_{i,k}$, $\widetilde{y}_{i,k}$.

II. Optimization over complex decision variables

In this section we give a brief overview of the technicalities involved with equality-constrained optimization over complex decision variables. We first note that in the context of minimization over complex decision variables, the objective function must be real ($f : \mathbb{C}^d \to \mathbb{R} : \boldsymbol{x} \mapsto f(\boldsymbol{x}), d \in \mathbb{Z}_+$). Indeed, for the optimization problem to be well-defined, $f(\boldsymbol{x})$ must be such that there exists an ordering on its function values[1]: one has to be able to conclude whether a solution $\boldsymbol{x}_1$ performs *better* than another solution $\boldsymbol{x}_2$ by means of the objective function value, e.g., $f(\boldsymbol{x}_1) < f(\boldsymbol{x}_2)$.

The first-order necessary conditions for optimality (FONC) of an optimization problem are obtained via the first-order derivatives of the corresponding Lagrangian. The *Cauchy–Riemann equations* serve as a necessary and sufficient condition for a function to be *analytic*, which means that its derivative is well defined for all points in the complex domain. Since real-valued objective functions, except for $f(\boldsymbol{x}) = c \in \mathbb{R}$, do not satisfy the Cauchy–Riemann equations, they are not complex differentiable.

Thus, we need a manner of redefining differentiation of a real-valued function $f(\boldsymbol{x})$ over complex variables $\boldsymbol{x} \in \mathbb{C}^d$. The most straightforward way of doing this, is by decoupling the derivatives w.r.t. the real and the imaginary parts, such that the real-valued objective function $f(\boldsymbol{x})$ can be interpreted as a function of two independent real variables $f(\boldsymbol{x}^{\mathrm{Re}}, \boldsymbol{x}^{\mathrm{Im}})$. This approach makes the problem completely real-valued, allowing for the use of real differential calculus to formulate the FONC for optimality.

The aforementioned reformulation of the optimization problem over complex variables into a real-valued problem is, however, often impractical, since it tends to obscure or destroy the structure of the original complex-variable problem.

[1]Even though it would be possible to impose an ordering on complex numbers which allows for a convenient comparison between two complex numbers, concepts such as the gradient and higher order derivatives would lose their meaning. The problem is that, although the complex numbers can be ordered in various ways, they cannot be made into an ordered field with the usual addition and multiplication operators [14].

An alternative approach involves the use of CR-calculus, also referred to as *Wirtinger derivatives* [14], which provides an equivalent but often more elegant formulation of the FONC. This approach is based on the observation that a function $f(\boldsymbol{x}^{\mathrm{Re}}, \boldsymbol{x}^{\mathrm{Im}})$ that is analytic over the vector space $\mathbb{R}^{d\times 2}$, is also analytic over the vector space $\{(\boldsymbol{x}, \overline{\boldsymbol{x}})\} \subset \mathbb{C}^{d\times 2}$.

For such a *polyanalytic* function $f(\boldsymbol{x}, \overline{\boldsymbol{x}})$ the Wirtinger derivatives towards $\boldsymbol{x}$ and $\overline{\boldsymbol{x}}$ are defined via the chain rule:

$$\frac{\partial f(\boldsymbol{x}, \overline{\boldsymbol{x}})}{\partial \boldsymbol{x}} = \frac{\partial f(\boldsymbol{x}^{\mathrm{Re}}, \boldsymbol{x}^{\mathrm{Im}})}{\partial \boldsymbol{x}^{\mathrm{Re}}} \frac{\partial \boldsymbol{x}^{\mathrm{Re}}}{\partial \boldsymbol{x}} + \frac{\partial f(\boldsymbol{x}^{\mathrm{Re}}, \boldsymbol{x}^{\mathrm{Im}})}{\partial \boldsymbol{x}^{\mathrm{Im}}} \frac{\partial \boldsymbol{x}^{\mathrm{Im}}}{\partial \boldsymbol{x}},$$
$$\frac{\partial f(\boldsymbol{x}, \overline{\boldsymbol{x}})}{\partial \overline{\boldsymbol{x}}} = \frac{\partial f(\boldsymbol{x}^{\mathrm{Re}}, \boldsymbol{x}^{\mathrm{Im}})}{\partial \boldsymbol{x}^{\mathrm{Re}}} \frac{\partial \boldsymbol{x}^{\mathrm{Re}}}{\partial \overline{\boldsymbol{x}}} + \frac{\partial f(\boldsymbol{x}^{\mathrm{Re}}, \boldsymbol{x}^{\mathrm{Im}})}{\partial \boldsymbol{x}^{\mathrm{Im}}} \frac{\partial \boldsymbol{x}^{\mathrm{Im}}}{\partial \overline{\boldsymbol{x}}},$$

which in practice boils down to differentiation of $f(\boldsymbol{x}, \overline{\boldsymbol{x}})$ with respect to $\boldsymbol{x}$ (resp. $\overline{\boldsymbol{x}}$), while considering the variable $\overline{\boldsymbol{x}}$ (resp. $\boldsymbol{x}$) as a constant, i.e., $\boldsymbol{x}$ and $\overline{\boldsymbol{x}}$ are treated as independent variables for the purpose of differentiation.

Though, one must be careful when working with constrained optimization problems over complex variables [14], [15]. To construct the Lagrangian when using Wirtinger derivatives, the original constraint as well as its complex conjugate must be incorporated into the Lagrangian using a single set of complex-conjugated Lagrange multipliers.

III. Complex Riemannian SVD (RiSVD)

A. Model-compliance

Writing out (1) for all $k = 0, \ldots, N-n-1$, illustrates that constraint (2b) of the realization problem can be expressed as

$$\begin{bmatrix} \widehat{\boldsymbol{Y}}_1 \\ \widehat{\boldsymbol{Y}}_2 \\ \vdots \\ \widehat{\boldsymbol{Y}}_p \end{bmatrix} \begin{bmatrix} \boldsymbol{a}_{\mathrm{tr}} \\ 1 \end{bmatrix} = \begin{bmatrix} \boldsymbol{T_a} & & & \\ & \boldsymbol{T_a} & & \\ & & \ddots & \\ & & & \boldsymbol{T_a} \end{bmatrix} \begin{bmatrix} \widehat{\boldsymbol{y}}_1 \\ \widehat{\boldsymbol{y}}_2 \\ \vdots \\ \widehat{\boldsymbol{y}}_p \end{bmatrix} = \boldsymbol{0}, \qquad (3)$$

where $\widehat{\boldsymbol{Y}}_i \in \mathbb{C}^{(N-n)\times(n+1)}$ is the Hankel matrix constructed from the elements of $\widehat{\boldsymbol{y}}_i$, and $\boldsymbol{T_a} \in \mathbb{C}^{(N-n)\times N}$ is a banded-Toeplitz matrix, where the first row of $\boldsymbol{T_a}$ is given by the model parameters appended with $N-n-1$ zeros: $[\boldsymbol{a}_{\mathrm{tr}}^{\mathsf{T}}\ 1\ 0\ \cdots\ 0]$, and all elements below the diagonal are zero. The subscript $\boldsymbol{a}$ denotes the vector $\boldsymbol{a} = [\boldsymbol{a}_{\mathrm{tr}}^{\mathsf{T}}\ 1]^{\mathsf{T}}$ generating the rows of $\boldsymbol{T_a}$. Notice the equality between the Hankel-vector products and the (banded) Toeplitz-vector products in (3). This reformulation follows from the Hankel/Toeplitz structure of the involved matrices and will be used extensively throughout this manuscript.

Relation (3) illustrates that the model parameters $\boldsymbol{a}$ associated to a known sequence of model-compliant output data can be retrieved via the null space of the model-compliant data block-Hankel matrix: $\widehat{\boldsymbol{Y}} = [\widehat{\boldsymbol{Y}}_1^{\mathsf{T}}\ \cdots\ \widehat{\boldsymbol{Y}}_p^{\mathsf{T}}]^{\mathsf{T}} \in \mathbb{C}^{p(N-n)\times(n+1)}$. Conversely, when the model parameters $\boldsymbol{a}$ are known, the *behavior* of the model[2] corresponds to the (pn)-dimensional null space of the block-diagonal matrix constructed from $\boldsymbol{T_a}$.

[2]This is the set of all model-compliant data sequences.

The given data $\boldsymbol{y}$, however, are not compliant with the model class under consideration, such that the given data block-Hankel matrix $\boldsymbol{Y} = [\boldsymbol{Y}_1^\mathsf{T} \ \cdots \ \boldsymbol{Y}_p^\mathsf{T}]^\mathsf{T} \in \mathbb{C}^{p(N-n)\times(n+1)}$, where each $\boldsymbol{Y}_i$ is a Hankel matrix, is of full column rank[3]:

$$\operatorname{rank}(\boldsymbol{Y}) = n + 1.$$

The identification problem (2) corresponds to a structured low-rank approximation problem: for a given data block-Hankel matrix $\boldsymbol{Y}$ that is of full column-rank, i.e., containing data that is not compliant with the model class under consideration, one wants to identify the best approximating, in a (weighted) least squares sense, low-rank block-Hankel matrix $\widehat{\boldsymbol{Y}}$. This rank-deficiency $\operatorname{rank}(\widehat{\boldsymbol{Y}}) \leq n$ is enforced by the constraint (2b). If $\operatorname{rank}(\widehat{\boldsymbol{Y}}) = n$, the model parameters corresponding to the model-compliant data $\widehat{\boldsymbol{y}}$ are unique.

B. Data optimality

We approach the realization problem (2) by first rewriting the constraints (2b) in terms of the Hankel matrices, as in (3), and constructing the Lagrangian, for which we rely on the concepts presented in Section II.

$$\mathcal{L}(\boldsymbol{a}_{\mathrm{tr}}, \widehat{\boldsymbol{y}}, \boldsymbol{\ell}) = \sum_{i=1}^{p} \Big[(\boldsymbol{y}_i - \widehat{\boldsymbol{y}}_i)^\mathsf{H}(\boldsymbol{y}_i - \widehat{\boldsymbol{y}}_i) + \boldsymbol{\ell}_i^\mathsf{H} \boldsymbol{T}_{\boldsymbol{a}} \widehat{\boldsymbol{y}}_i + \boldsymbol{\ell}_i^\mathsf{T} \overline{\boldsymbol{T}_{\boldsymbol{a}} \widehat{\boldsymbol{y}}_i} \Big],$$

where the vector $\boldsymbol{\ell} = [\boldsymbol{\ell}_1^\mathsf{T} \ \ldots \ \boldsymbol{\ell}_p^\mathsf{T}]^\mathsf{T} \in \mathbb{C}^{p(N-n)}$ contains the Lagrange multipliers. The system of equations that characterizes the first-order optimal solutions follows from equating the partial derivatives of the Lagrangian to zero:

$$\partial \mathcal{L} / \partial \overline{\boldsymbol{\ell}_i} = \boldsymbol{T}_{\boldsymbol{a}} \widehat{\boldsymbol{y}}_i = \boldsymbol{0}, \quad \forall i \in \{1, \ldots, p\} \tag{4}$$

$$\partial \mathcal{L} \Big/ \partial \overline{\widehat{\boldsymbol{y}}_i} = \widehat{\boldsymbol{y}}_i - \boldsymbol{y}_i + \boldsymbol{T}_{\boldsymbol{a}}^\mathsf{H} \boldsymbol{\ell}_i = \boldsymbol{0}, \quad \forall i \in \{1, \ldots, p\} \tag{5}$$

$$\partial \mathcal{L} / \partial \overline{\boldsymbol{a}_{\mathrm{tr}}} = \sum_{i=1}^{p} \widehat{\boldsymbol{Y}}_i^\mathsf{H} \boldsymbol{\ell}_i = \boldsymbol{0}. \tag{6}$$

Since $\mathcal{L}$ is purely real, the partial derivatives w.r.t. $\boldsymbol{\ell}_i$, $\widehat{\boldsymbol{y}}_i$, and $\boldsymbol{a}_{\mathrm{tr}}$ correspond to the complex conjugates of (4), (5), and (6), respectively.

Equating the partial derivatives of the Lagrangian w.r.t. the model-compliant data to zero (cfr. (5)) illustrates that for each output i, the misfits $\widetilde{\boldsymbol{y}}_i$ lie in the row space of the complex conjugate of the Toeplitz matrix $\boldsymbol{T}_{\boldsymbol{a}}$

$$\begin{aligned} -(\boldsymbol{y}_i - \widehat{\boldsymbol{y}}_i) + \boldsymbol{T}_{\boldsymbol{a}}^\mathsf{H} \boldsymbol{\ell}_i = \boldsymbol{0} \\ \iff \widetilde{\boldsymbol{y}}_i = \boldsymbol{T}_{\boldsymbol{a}}^\mathsf{H} \boldsymbol{\ell}_i. \end{aligned} \tag{7}$$

Combining this with the constraints (3) and $\boldsymbol{y}_i = \widehat{\boldsymbol{y}}_i + \widetilde{\boldsymbol{y}}_i$ gives

$$\begin{aligned} \boldsymbol{T}_{\boldsymbol{a}} \widehat{\boldsymbol{y}}_i = \boldsymbol{T}_{\boldsymbol{a}} (\boldsymbol{y}_i - \widetilde{\boldsymbol{y}}_i) = \boldsymbol{0} \\ \iff \boldsymbol{T}_{\boldsymbol{a}} \boldsymbol{y}_i = \boldsymbol{T}_{\boldsymbol{a}} \widetilde{\boldsymbol{y}}_i \\ \iff \boldsymbol{T}_{\boldsymbol{a}} \boldsymbol{y}_i = \boldsymbol{T}_{\boldsymbol{a}} \boldsymbol{T}_{\boldsymbol{a}}^\mathsf{H} \boldsymbol{\ell}_i. \end{aligned}$$

[3]Remark that the matrix of given data $\boldsymbol{Y}$ has a non-trivial null space by construction when $p(N-n) < n+1$, such that $N \geq \lceil n + (n+1)/p \rceil$ is a necessary condition for the identification problem to be well-defined.

Writing this out for all outputs $i = 1, \ldots, p$ gives

$$\begin{bmatrix} \boldsymbol{T}_{\boldsymbol{a}} & & & \\ & \boldsymbol{T}_{\boldsymbol{a}} & & \\ & & \ddots & \\ & & & \boldsymbol{T}_{\boldsymbol{a}} \end{bmatrix} \begin{bmatrix} \widehat{\boldsymbol{y}}_1 \\ \widehat{\boldsymbol{y}}_2 \\ \vdots \\ \widehat{\boldsymbol{y}}_p \end{bmatrix} = \boldsymbol{D}_{\boldsymbol{a}} \begin{bmatrix} \boldsymbol{\ell}_1 \\ \vdots \\ \boldsymbol{\ell}_p \end{bmatrix}, \tag{8}$$

where the square matrix $\boldsymbol{D}_{\boldsymbol{a}} \in \mathbb{C}^{p(N-n)\times p(N-n)}$ corresponds to a block-diagonal matrix of p blocks:

$$\boldsymbol{D}_{\boldsymbol{a}} = \operatorname{blockdiag}\Big(\boldsymbol{T}_{\boldsymbol{a}} \boldsymbol{T}_{\boldsymbol{a}}^\mathsf{H}, \boldsymbol{T}_{\boldsymbol{a}} \boldsymbol{T}_{\boldsymbol{a}}^\mathsf{H}, \ldots, \boldsymbol{T}_{\boldsymbol{a}} \boldsymbol{T}_{\boldsymbol{a}}^\mathsf{H} \Big).$$

Using (3) we can rewrite (8) as,

$$\begin{bmatrix} \boldsymbol{Y}_1 \\ \vdots \\ \boldsymbol{Y}_p \end{bmatrix} \begin{bmatrix} \boldsymbol{a}_{\mathrm{tr}} \\ 1 \end{bmatrix} = \boldsymbol{D}_{\boldsymbol{a}} \boldsymbol{\ell}, \tag{9}$$

where $\boldsymbol{\ell} = [\boldsymbol{\ell}_1^\mathsf{T}, \ldots, \boldsymbol{\ell}_p^\mathsf{T}]^\mathsf{T}$. It follows from (8) that the optimal Lagrange multipliers $\boldsymbol{\ell}_i$ correspond to

$$\boldsymbol{\ell}_i = (\boldsymbol{T}_{\boldsymbol{a}} \boldsymbol{T}_{\boldsymbol{a}}^\mathsf{H})^{-1} \boldsymbol{T}_{\boldsymbol{a}} \boldsymbol{y}_i$$

such that the optimal misfits $\widetilde{\boldsymbol{y}}_i$ are obtained via the orthogonal projection of the given data $\boldsymbol{y}_i$ onto $\operatorname{row}(\boldsymbol{T}_{\boldsymbol{a}})$:

$$\widetilde{\boldsymbol{y}}_i = \boldsymbol{T}_{\boldsymbol{a}}^\mathsf{H} (\boldsymbol{T}_{\boldsymbol{a}} \boldsymbol{T}_{\boldsymbol{a}}^\mathsf{H})^{-1} \boldsymbol{T}_{\boldsymbol{a}} \boldsymbol{y}_i.$$

C. Model optimality

Optimality of the model parameters $\boldsymbol{a}$ is obtained when we equate the partial derivatives of the Lagrangian w.r.t. the model-parameters (6) to zero

$$\begin{aligned} \sum_{i=1}^{p} \widehat{\boldsymbol{Y}}_i^\mathsf{H} \boldsymbol{\ell}_i = \sum_{i=1}^{p} \Big(\boldsymbol{Y}_i^\mathsf{H} - \widetilde{\boldsymbol{Y}}_i^\mathsf{H} \Big) \boldsymbol{\ell}_i = \boldsymbol{0} \\ \iff \begin{bmatrix} \boldsymbol{Y}_1^\mathsf{H} & \cdots & \boldsymbol{Y}_2^\mathsf{H} \end{bmatrix} \begin{bmatrix} \boldsymbol{\ell}_1 \\ \vdots \\ \boldsymbol{\ell}_p \end{bmatrix} = \sum_{i=1}^{p} \boldsymbol{T}_{\boldsymbol{\ell}_i} \overline{\widetilde{\boldsymbol{y}}_i}. \end{aligned}$$

Use now that $\overline{\widetilde{\boldsymbol{y}}_i} = \boldsymbol{T}_{\boldsymbol{a}}^\mathsf{T} \overline{\boldsymbol{\ell}_i}$ which follows from the complex conjugate of (7) and $\boldsymbol{T}_{\boldsymbol{a}}^\mathsf{T} \overline{\boldsymbol{\ell}_i} = \boldsymbol{T}_{\boldsymbol{\ell}_i}^\mathsf{H} \boldsymbol{a}$, such that

$$\begin{bmatrix} \boldsymbol{Y}_1^\mathsf{H} & \cdots & \boldsymbol{Y}_2^\mathsf{H} \end{bmatrix} \boldsymbol{\ell} = \boldsymbol{D}_{\boldsymbol{\ell}} \boldsymbol{a}, \tag{10}$$

where the square matrix $\boldsymbol{D}_{\boldsymbol{\ell}} \in \mathbb{C}^{(n+1)\times(n+1)}$ corresponds to

$$\boldsymbol{D}_{\boldsymbol{\ell}} = \sum_{i=1}^{p} \boldsymbol{T}_{\boldsymbol{\ell}_i} \boldsymbol{T}_{\boldsymbol{\ell}_i}^\mathsf{H}.$$

D. Complex Riemannian SVD (RiSVD)

Combining (9) with (10) leads to the following system:

$$\begin{aligned} \boldsymbol{Y} \boldsymbol{a} &= \boldsymbol{D}_{\boldsymbol{a}} \boldsymbol{\ell}, \\ \boldsymbol{Y}^\mathsf{H} \boldsymbol{\ell} &= \boldsymbol{D}_{\boldsymbol{\ell}} \boldsymbol{a}. \end{aligned}$$

Substituting $\boldsymbol{\ell}$ via $\boldsymbol{\ell} = \tau \boldsymbol{u}$, with $\tau \in \mathbb{R}$ such that $\boldsymbol{u}^\mathsf{H} \boldsymbol{D}_{\boldsymbol{a}} \boldsymbol{u} = 1$ and $\boldsymbol{D}_{\boldsymbol{\ell}} = \tau^2 \boldsymbol{D}_{\boldsymbol{u}}$, we obtain the set of equations:

$$\begin{aligned} \boldsymbol{Y} \boldsymbol{a} = \boldsymbol{D}_{\boldsymbol{a}} \boldsymbol{u} \tau, \qquad \boldsymbol{a} = \begin{bmatrix} \boldsymbol{a}_{\mathrm{tr}} \\ 1 \end{bmatrix}, \\ \boldsymbol{Y}^\mathsf{H} \boldsymbol{\ell} = \boldsymbol{D}_{\boldsymbol{u}} \boldsymbol{a} \tau, \quad \boldsymbol{u}^\mathsf{H} \boldsymbol{D}_{\boldsymbol{a}} \boldsymbol{u} = 1. \end{aligned} \tag{11}$$

This is a nonlinear generalized SVD with $\boldsymbol{D_a}$ and $\boldsymbol{D_u}$ positive definite weighting matrices, quadratic in $\boldsymbol{a}$ and $\boldsymbol{u}$, respectively. On the basis of our analysis, we conclude that the original real Riemannian SVD (RiSVD) generalizes to the complex plane by replacing the transposes with Hermitian conjugates. The value of τ^2 is equal to the objective function, i.e., the squared norm of the misfit $\|\widetilde{\boldsymbol{y}}\|_2^2$, just as in [11].

In other words, the identification problem (2) can be solved in a locally optimal way by computing the triplet $(\boldsymbol{a}, \tau, \boldsymbol{u}) \in \mathbb{C}^{n+1} \times \mathbb{R} \times \mathbb{C}^{p(N-n)}$ that solves the RiSVD (11) with smallest possible τ^2. The corresponding model-compliant data $\widehat{\boldsymbol{y}}$ can be obtained from the triplet $(\boldsymbol{a}, \tau, \boldsymbol{u})$ via

$$\begin{bmatrix} \widehat{\boldsymbol{y}}_1 \\ \vdots \\ \widehat{\boldsymbol{y}}_p \end{bmatrix} = \begin{bmatrix} \boldsymbol{y}_1 \\ \vdots \\ \boldsymbol{y}_p \end{bmatrix} - \tau \begin{bmatrix} \boldsymbol{T}_{\boldsymbol{a}}^{\mathsf{H}} & & \\ & \ddots & \\ & & \boldsymbol{T}_{\boldsymbol{a}}^{\mathsf{H}} \end{bmatrix} \boldsymbol{u}. \tag{12}$$

IV. An inverse-iteration method

To solve for a minimizing triplet $(\boldsymbol{a}, \tau, \boldsymbol{u})$ of the real-valued RiSVD, the standard variable metric inverse iteration algorithm can be used [11]. With a few minor adjustments, this algorithm generalizes to the complex-valued RiSVD (11): All transposes in the original algorithm should be changed to Hermitian transposes; and to ensure uniqueness of equivalent obtained triplets $\boldsymbol{a}^{(k)}$ and $\boldsymbol{u}^{(k)}$ are projected such that $a_0^{(k)} = 1$ (line 13 and 14). Algorithm 1 shows the modified algorithm. Note that all variables in Algorithm 1 are complex.

Like alternating least squares (ALS) methods, this algorithm iteratively solves the two equations in the first column of (11) by linearizing them freezing $\boldsymbol{D_u}$ and $\boldsymbol{D_a}$ for the current values of $\boldsymbol{u}$ and $\boldsymbol{a}$. In each subsequent iteration, the metrics $\boldsymbol{D_u}$ and $\boldsymbol{D_a}$ are updated with the new values of the intermediate solutions $\boldsymbol{u}^{(k)}$ and $\boldsymbol{a}^{(k)}$ and the same (linearized) equations are solved again. The algorithm splits $\boldsymbol{u}$ into two orthogonal components $\boldsymbol{Q}_1\boldsymbol{z}$ and $\boldsymbol{Q}_2\boldsymbol{w}$ and uses the (complex) QR-decomposition of $\boldsymbol{Y}$ to more efficiently compute the inverse on line 6 of the algorithm. The output of the algorithm depends on the initial guesses $\boldsymbol{u}^{(k)}$ and $\boldsymbol{a}^{(k)}$, which makes this a heuristic approach. Convergence is tested by measuring the difference between subsequent values $\tau^{(k)}$.

V. Numerical experiments

This section discusses two numerical experiments of complex realization problems to illustrate Algorithm 1.

A. Nuclear magnetic resonance (NMR) modeling

Complex signals are prevalent in nuclear magnetic resonance (NMR) modeling, where they allow storing phase information obtained via quadrature detection. We closely follow an experiment described in [6], where a signal produced by an nth-order autonomous single-output system is modeled as:

$$y_{\text{exact},k} = \sum_{m=1}^{n} A_m e^{\mathrm{j}(\varphi_0+\varphi_m)} e^{(-d_m+\mathrm{j}2\pi f_m)t_k} \tag{13}$$

Algorithm 1. Variable metric inverse iteration algorithm on $\mathbb{C}$, based on [11].

Input: Initial guess $\boldsymbol{a}^{(0)}$, $\boldsymbol{u}^{(0)}$;
$\boldsymbol{Q} \in \mathbb{C}^{p(N-n)\times p(N-n)}, \boldsymbol{R} \in \mathbb{C}^{p(N-n)\times(n+1)} \leftarrow \mathrm{QR}(\boldsymbol{Y})$
1 $\boldsymbol{Q}_1, \boldsymbol{Q}_2 \leftarrow \boldsymbol{Q}_{[1:n+1]}, \boldsymbol{Q}_{[n+2:p(N-n)]}$
`/* subscript denotes a range of columns */`
2 $k \leftarrow 0$
3 **repeat**
4 $\quad k \leftarrow k+1$
5 $\quad \boldsymbol{z}^{(k)} \leftarrow \boldsymbol{R}^{-\mathsf{H}} \boldsymbol{D}_{\boldsymbol{u}^{(k-1)}} \boldsymbol{a}^{(k-1)}$
6 $\quad \boldsymbol{w}^{(k)} \leftarrow -\left(\boldsymbol{Q}_2^{\mathsf{H}} \boldsymbol{D}_{\boldsymbol{a}^{(k-1)}} \boldsymbol{Q}_2\right)^{-1} \left(\boldsymbol{Q}_2^{\mathsf{H}} \boldsymbol{D}_{\boldsymbol{a}^{(k-1)}} \boldsymbol{Q}_1\right) \boldsymbol{z}^{(k)}$
7 $\quad \boldsymbol{u}^{(k)} \leftarrow \boldsymbol{Q}_1 \boldsymbol{z}^{(k)} + \boldsymbol{Q}_2 \boldsymbol{w}^{(k)}$
8 $\quad \boldsymbol{u}^{(k)} \leftarrow \frac{\boldsymbol{u}^{(k)}}{\|\boldsymbol{u}^{(k)}\|_2}$
9 $\quad \boldsymbol{a}^{(k)} \leftarrow \boldsymbol{R}^{-1} \boldsymbol{Q}_1^{\mathsf{H}} \boldsymbol{D}_{\boldsymbol{a}^{(k-1)}} \boldsymbol{u}^{(k)}$
10 $\quad \tau^{(k)} \leftarrow \left\|\boldsymbol{a}^{(k)}\right\|_2$
11 $\quad \boldsymbol{a}^{(k)} \leftarrow \frac{\boldsymbol{a}^{(k)}}{\tau^{(k)}}$
12 **until** *convergence*
13 $\boldsymbol{u}^{(k)} \leftarrow \boldsymbol{u}^{(k)} a_0^{(k)}$
14 $\boldsymbol{a}^{(k)} \leftarrow \boldsymbol{a}^{(k)} / a_0^{(k)}$

TABLE I
Exact parameter values of the simulated NMR signal used in (13) in experiment 1, as also used in [6, Table 2].

m	f_m [Hz]	d_m [rad/s]	A_m [1]	φ_m [rad]
1	-1379	208	6.1	$15\pi/180$
2	-685	256	9.9	$15\pi/180$
3	-271	197	6.0	$15\pi/180$
4	353	117	2.8	$15\pi/180$
5	478	808	17.0	$15\pi/180$

where $t_k = kT_\mathrm{s}$ with T_s the sampling period. The frequencies f_m and damping factors d_m can be retrieved via the roots z_m of $\boldsymbol{a}(z)$, i.e., the degree n polynomial of model parameters (1).

Experiment 1: The performance of the method is tested using simulated data obtained from a model with parameters A_m, φ_m, d_m, and f_m as shown in Table I, and $\varphi_0 = 0$. Note that the frequencies f_4 and f_5 lie close to each other, making the estimation problem quite ill conditioned.

The model is evaluated for $N = 128$ data points, uniformly sampled with sampling time $T_\mathrm{s} = 10^{-4}$ s. The data sequence is perturbed with complex zero mean Gaussian noise $\varepsilon_k \in \mathbb{C}$ with variance $4\nu^2$, i.e., where

$$\varepsilon_k = \varepsilon_k^{\mathrm{Re}} + \mathrm{j}\varepsilon_k^{\mathrm{Im}}, \qquad \varepsilon_k^{\mathrm{Re}}, \varepsilon_k^{\mathrm{Im}} \sim \mathcal{N}\left(0, \nu^2\right). \tag{14}$$

The best total least squares (TLS) estimator of the model parameters $\boldsymbol{a}_{\mathrm{TLS}}$ is used to determine an initial guess for the inverse iteration algorithm (Algorithm 1): (1) $\boldsymbol{a}^{(0)}$ is taken as the TLS estimate $\boldsymbol{a}_{\mathrm{TLS}}$; (2) $\boldsymbol{u}^{(0)}$ is then calculated as $\boldsymbol{u}^{(0)} = \left(\boldsymbol{T}_{\boldsymbol{a}^{(0)}}^{\mathsf{H}}\right)^{\dagger} (\boldsymbol{y} - \widehat{\boldsymbol{y}}_{\mathrm{TLS}})$, where $\widehat{\boldsymbol{y}}_{\mathrm{TLS}}$[4] is the model-compliant data as estimated using TLS.

Each of the obtained solutions is a local minimum of the realization problem (2). Fig. 2 shows the distribution of the misfits, where we observe that they are larger for increasing

[4]Note that $\widehat{\boldsymbol{y}}_{\mathrm{TLS}}$ is not a critical point of (2), since it disregards the Hankel structure of the given data matrix $\boldsymbol{Y}$ when reducing its rank.

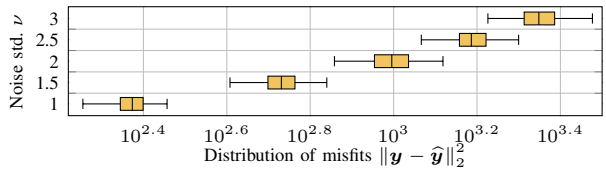

Fig. 2. Distribution of misfits for 200 noisy realizations for various noise levels corresponding to Experiment 1.

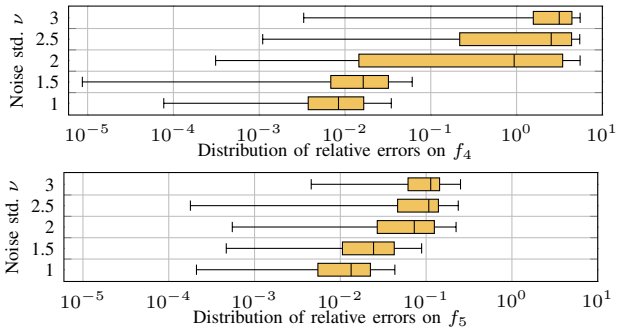

Fig. 3. Relative errors on f_4 and f_5 for 200 noisy realizations for various noise levels corresponding to Experiment 1.

noise levels. For larger noise levels, the given data $\boldsymbol{y}$ stray further away from the *model-compliant data space*. Since this space is merely a small subspace of the large ambient space $\mathbb{C}^{pN}$, it is not unexpected to observe these increasing misfits $\|\widetilde{\boldsymbol{y}}\|$ after projection of the given data onto this space.

Figs. 3 and 4 show the relative errors on the hard to estimate frequencies f_4 and f_5 and damping factors d_4 and d_5, respectively. It is clear from Fig. 3 that for larger noise levels f_4 is not correctly estimated. This is due to the RiSVD method overfitting on the noise and consequently interpreting the contributions of f_4 and f_5 as contributions done by only a single frequency. Overfitting on the noise is a natural consequence of the objective function (2).

B. Direction of arrival (DOA) estimation

In a second experiment we relate the autonomous realization problem to a direction of arrival (DOA) estimation problem. Estimating the DOA is a common problem in radar, sonar, and wireless communication applications [10], [16].

Consider a setup of p sensors, evenly distributed along a

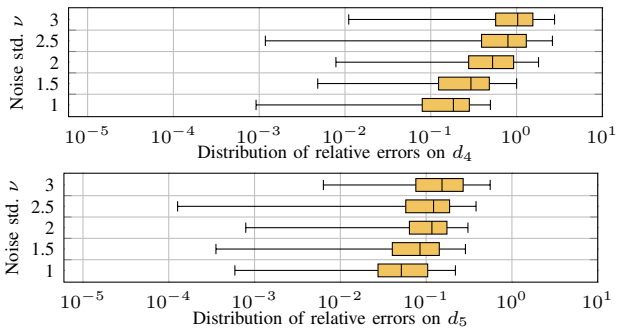

Fig. 4. Relative errors on d_4 and d_5 for 200 noisy realizations for various noise levels corresponding to Experiment 1.

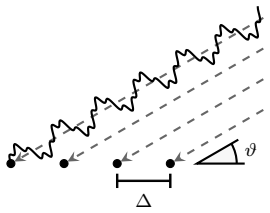

Fig. 5. A sensor array consisting of $p = 4$ sensors on a line receiving the same signal that arrives in an angle ϑ w.r.t. the sensor array. Each sensor is represented by a dot. The distance between two successive sensors is Δ.

line as illustrated in Fig. 5. A signal $s(t)$ is transmitted and received by the sensor array under an angle ϑ, where $s(t)$ is modeled as a sum of n constant amplitude complex exponentials:

$$s(t) = \sum_{m=1}^{n} R_m e^{\mathrm{j}\psi_m} e^{\mathrm{j}2\pi f_m t}.$$

With $R_m, \psi_m, f_m \in \mathbb{R}$. The signal source is assumed to be far enough such that the DOA ϑ is virtually the same for each sensor. The ith antenna receives a phase-shifted discrete-time version of $s(t)$ perturbed by zero mean Gaussian measurement noise:

$$y_{i,k} = \sum_{m=1}^{n} R_m e^{\mathrm{j}\psi_m} e^{\mathrm{j}2\pi f_m (kT_\mathrm{s}+\varphi_0+\varphi_i)} + \varepsilon_{i,k}. \tag{15}$$

We assume φ_0 to be zero. The phase-shift of the ith sensor is then given by:

$$\varphi_i = i\frac{\Delta\cos(\vartheta)}{c} \tag{16}$$

where c is the speed of light and Δ is the distance between two successive sensors. After calculating the best fitting model parameters $\boldsymbol{a}$ corresponding to the received data $\boldsymbol{y}_i$ (15), the corresponding $\widehat{R}_m$, $\widehat{\psi}_m$ and $\widehat{f}_m$ can be determined and consequently the DOA ϑ can be estimated using (16).

Experiment 2: We consider a setup of $p = 4$ sensors, where the distance between two successive sensors is $\Delta = 250\,\mathrm{m}$ and the (unknown) DOA $\vartheta = \pi/4$. We generate 200 different signals by randomly generating 200 sets of $\boldsymbol{R}, \boldsymbol{f} \in \mathbb{R}^n$ and $\boldsymbol{\psi} = \boldsymbol{0}$ and evaluate the model (15) for $N = 128$ samples, where $T_\mathrm{s} = 1\,\mu\mathrm{s}$. To ensure the frequencies f_m being sufficiently distinct, they are drawn from a normal distribution $\mathcal{N}(\frac{m-1}{2nT_\mathrm{s}}, \frac{1}{(2nT_\mathrm{s})^2})$. The amplitudes R_m are drawn from a uniform distribution on the range $[5, 15]$. The experiment is performed for different signal to noise ratios $\mathrm{SNR} = 0, 2, \ldots, 10$ dB. For each SNR, zero mean Gaussian noise with variance $4\nu^2$ (14) is added, such that $\mathrm{SNR} = 10\log_{10}\left(P_\mathrm{avg}/4\nu^2\right)$ where $P_\mathrm{avg} = \|y_\mathrm{exact}\|_2^2/pN$ is the average power of the noiseless signal. The resulting data is gathered in a vector $\boldsymbol{y}$ and structured in a Hankel matrix $\boldsymbol{Y}$. Using Algorithm 1, the optimal RiSVD triplet $(\boldsymbol{u}, \tau, \boldsymbol{a})$ is determined with corresponding model-compliant data $\widehat{\boldsymbol{y}}$ via (12). The parameter estimates $\widehat{R}_m, \widehat{\psi}_m, \widehat{f}_m$ corresponding to the model-compliant data $\widehat{\boldsymbol{y}}$ can be retrieved via the model parameters $\boldsymbol{a}$, and subsequently the DOA ϑ can be estimated.

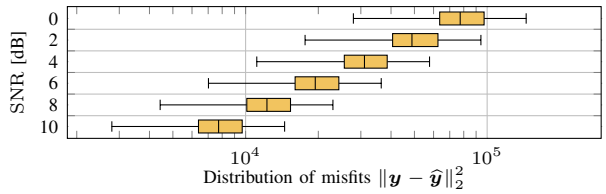

Fig. 6. Distribution of misfits for 200 different noisy realizations for various noise levels corresponding to Experiment 2.

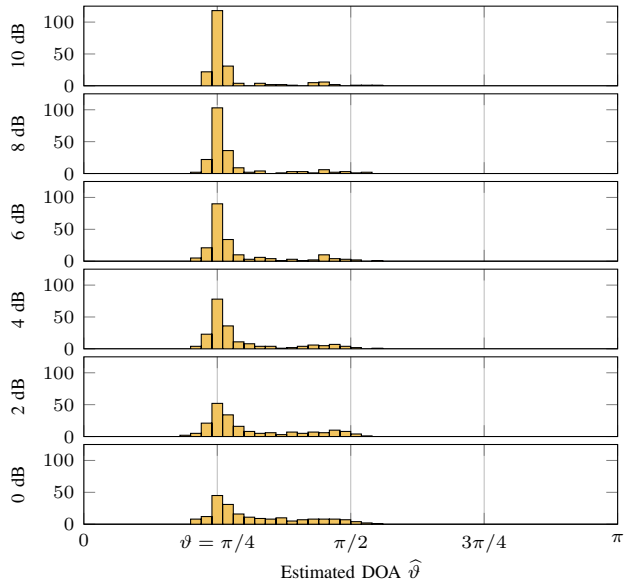

Fig. 7. Histograms of the estimated DOA $\widehat{\vartheta}$ for 200 different noisy signals for $\mathrm{SNR} = 0, 2, \ldots, 10$ dB corresponding to Experiment 2.

Fig. 6 shows the distribution of the misfits. Similarly as in Experiment 1, we observe increasing misfits for increasing noise levels. Fig. 7 shows histograms of the estimated DOA $\widehat{\vartheta}$ of the 200 different noisy signals for each of the various noise levels $\mathrm{SNR} = 0, 2, \ldots, 10$ dB. The histograms are constructed using bins of width $\pi/50$ rad. The estimated DOA shows a peak around the true DOA $\vartheta = \pi/4$ for all noise levels, where the peak is more pronounced for smaller noise levels. This experiment shows that for smaller noise levels the RiSVD method is able to estimate ϑ within a reasonable accuracy, and even for larger noise levels the estimations still show a peak near the true DOA ϑ.

VI. Conclusions and Future Work

We show that the (locally) optimal solutions of the complex LS realization problem follow from a nonlinear generalized singular value decomposition (Riemannian SVD) over the complex field and that with few minor adjustments the standard variable metric inverse iteration algorithm can be used to solve for minimizing singular triplets. The numerical experiments illustrate the use of the realization algorithm for two experiment setups. This work helps bridge the gap between real- and complex-valued modeling, offering new tools in signal processing, control theory, and related fields where complex data and models are prevalent.

References

[1] L. Ljung, *System Identification: Theory for the User*, 2nd ed., ser. Prentice-Hall Information and System Sciences Series. Upper Saddle River, NJ, USA: Prentice-Hall, 1999.

[2] P. Van Overschee and B. De Moor, *Subspace Identification for Linear Systems: Theory – Implementation – Applications*. Kluwer Academic Publishers, 1996.

[3] S. Lagauw, L. Vanpoucke, and B. De Moor, "Exact characterization of the global optima of least squares realization of autonomous LTI models as a multiparameter eigenvalue problem," in *Proc. of the 22nd European Control Conference (ECC)*, Stockholm, Sweden, Jun. 2024, pp. 3439–3444.

[4] U. Oberst, M. Scheicher, and I. Scheicher, *Linear Time-Invariant Systems, Behaviors and Modules*, ser. Differential-Algebraic Equations Forum. Springer, 2020.

[5] P. Stoica and R. L. Moses, *Spectral Analysis of Signals*. Pearson Prentice Hall, 2005.

[6] S. Vanhuffel, H. Chen, C. Decanniere, and P. Vanhecke, "Algorithm for time-domain nmr data fitting based on total least squares," *Journal of Magnetic Resonance, Series A*, vol. 110, no. 2, pp. 228–237, Oct. 1994.

[7] R. Pintelon and J. Schoukens, *System Identification: A Frequency Domain Approach.*, 2nd ed. Wiley-IEEE Press, 2012.

[8] C. Lee, H. Hasegawa, and S. Gao, "Complex-valued neural networks: A comprehensive survey," *IEEE/CAA Journal of Automatica Sinica*, vol. 9, no. 8, pp. 1406–1426, 2022.

[9] B. De Moor, "Least squares optimal realisation of autonomous LTI systems is an eigenvalue problem," *Communications in Information and Systems*, vol. 20, no. 2, pp. 163 – 207, 2020.

[10] R. Roy and T. Kailath, "ESPRIT-estimation of signal parameters via rotational invariance techniques," *IEEE Transactions on Acoustics, Speech, and Signal Processing*, vol. 37, no. 7, pp. 984–995, 1989.

[11] B. De Moor, "Structured total least squares and L_2 approximation problems," *Linear Algebra and its Applications*, vol. 188-189, pp. 10.1016/S1474–6670, 1993.

[12] G. H. Golub and V. Pereyra, "Separable nonlinear least squares: the variable projection method and its applications," *Inverse Problems*, vol. 19, no. 2, pp. R1–R26, 2003.

[13] I. Markovsky, J. Willems, S. Van Huffel, B. D. Moor, and R. Pintelon, "Application of structured total least squares for system identification and model reduction," *IEEE Transactions on Automatic Control*, vol. 50, no. 10, pp. 1490–1500, Oct. 2005.

[14] K. Kreutz-Delgado, "The complex gradient operator and the $\mathbb{CR}$-calculus," 2009. [Online]. Available: https://arxiv.org/abs/0906.4835

[15] W. T. Charles, *Discrete Random Signals and Statistical Signal Processing*, ser. Prentice-Hall signal processing series. Prentice Hall, 1992, vol. 1.

[16] A. M. Molaei, B. Zakeri, S. M. H. Andargoli, M. A. B. Abbasi, V. Fusco, and O. Yurduseven, "A comprehensive review of direction-of-arrival estimation and localization approaches in mixed-field sources scenario," *IEEE Access*, vol. 12, pp. 65 883–65 918, 2024.